UDC 551.511.6:551.551.2:551.584.4

A MODELING STUDY OF SEVERAL ASPECTS OF CANOPY FLOW

SUMNER BARR [1]
University of Utah, Salt Lake City, Utah

ABSTRACT

Several aspects of canopy flow are investigated. The problem of steady flow in a horizontally infinite canopy under neutral thermal stratification is treated theoretically. The resulting analytical model is then used as a boundary condition for a nonlinear numerical model designed to study transition regions near the leading and trailing edges of a canopy.

This model shows a wave effect downstream from a leading edge observed in the field and laboratory. A tendency for a splitting of the flow near a windward canopy edge is also brought out.

1. INTRODUCTION

Early observations of wind in vegetation-air layers revealed a characteristic velocity profile that showed a curvature reversal near the top of the vegetation and a region of low shear within the layer.

Agricultural requirements motivated the first quantitative attempts to model the turbulent transfer in the canopy environment. Theoretical contributions by Lemon et al. (1963) and Inoue (1963) treated steady-state flow in a horizontally homogeneous region The basic premise of the work is that there is a destruction of momentum by drag forces within the canopy layer and that the deceleration may be described by the differential equation

$$\frac{d\tau}{dz}=\rho CF(z)U^2(z) \tag{1}$$

where τ is turbulent stress; ρ is air density; C is the drag coefficient, a function of wind speed and leaf characteristics; F is leaf area density; U is mean wind speed; and z is height.

Turbulent stress τ has been related to the mean wind field through eddy viscosity hypotheses (Tan and Ling 1963) and through mixing length arguments (Inoue 1963, Cionco 1965).

Since the early measurements of wind profiles in vegetative canopies, the observational interests have developed along the lines of:

1. Equilibrium profiles of mean velocity in different types of canopies.
2. More sophisticated measurements, including turbulence spectra.
3. Diffusion of suspended material in the canopy environment.
4. Transition zone observations.
5. Laboratory model simulations.

Velocity profiles and turbulence intensity in agricultural crops are reported by Inoue (1963), Uchijima and Wright (1964), and Lemon et al. (1963). Mean wind, turbulence, and diffusion observations in tree forests have been carried out by Baynton et al. (1965), Morton (1968), and Raynor (1967). Allen (1968) has calculated mean wind speed profiles and turbulence spectra at various heights in a canopy.

Of very practical interest is the problem of flow in the transition regions at the windward and leeward ends of a canopy. This problem has received some attention through field and laboratory studies, but very little theoretical work has been done. Stearns (1964) made mean velocity profile observations within an artificial canopy made of Christmas trees mounted on a frozen lake. Investigators at Colorado State University at Fort Collins have gathered data from wind tunnel models of canopies and have observed transition regions as well as quasi-equilibrium flows. Plate and Quraishi (1965) measured mean speed profiles in and above several simplified canopies. Meroney (1968) reports observations of mean velocity, turbulence parameters, and concentration of a diffusing gas in the vicinity of model canopies.

A significant effect observed by Meroney in the leading edge transition zone is the tendency for the flow to be forced upward very near the leading edge and dip downward farther downstream. This same wave effect was noted in the field by Raynor (1967) who studied the diffusion of an aerosol tracer at the leading edge of a forest stand. Also, Raynor found an increase in the spread of aerosol with the forest. Shinn (1968) has assembled some observations from a leading edge zone of a deciduous forest and calculated horizontal and vertical wind components in the trunk space beneath the leaf crown. These estimates show the strongest upward component near the top portion of the trunk space at the leading edge.

A second feature that appears in each of the leading edge observations is a local maximum in the horizontal flow with the canopy. The velocity throughout the whole canopy region decreases into the canopy; but the decrease is slower in the lower half, thus giving rise to a weak jet. This has generally been ascribed to a splitting of the flow around the denser crown region that occupies the upper portion of the canopy. This, of course, is a physically

[1] Present affiliation: Physics Department, Drexel University, Philadelphia, Pa.

plausible explanation; but the phenomenon was also observed by Yano (1966) in a wind tunnel model consisting of simple pegs. In light of this, it is reasonable to look for further mechanisms contributing to the splitting effect.

The current study is directed toward the steady-state problem under neutral thermal stratification with interest focused on each of three zones:

1. A horizontally uniform zone; the mean flow is parallel and horizontal.
2. A leading edge transition zone where turbulence structure and mean flow are treated as two-dimensional variables (alongwind and vertical).
3. A two-dimensional trailing edge zone.

The uniform canopy is treated first, as it provides a boundary condition for the transition zone models. A model for the uniform canopy is derived from the Reynolds equation of motion, making use of mixing length hypotheses and a two-layer interaction hypothesis. The calculations for this model can be made analytically. The two-dimensional transition zone models are formulated in finite-difference equations and solved numerically. In addition to the canopy flow that represents an "inner" boundary condition, an outer boundary condition is selected to be a characteristic logarithmic velocity profile.

2. UNIFORM CANOPY MODEL

Our model for a uniform canopy will be formulated somewhat differently from previous models. We shall consider two interacting flow regimes. An outer boundary layer flow is not unlike that over a flat plate, except that the lower boundary condition is determined by continuity with the inner regime. The inner or canopy flow is characterized by a turbulence structure strongly affected by the large roughness elements. We shall consider it to be driven by the stress applied at canopy top by the outer velocity. The distribution of velocity in the canopy layer then depends on the turbulence structure within the region and the boundary conditions, continuity at the interface, and no-slip at the ground level.

The flow in each region satisfies the Reynolds form of the momentum conservation equations for an incompressible quasi-steady turbulent flow in two dimensions:

$$U\frac{\partial U}{\partial x}+W\frac{\partial U}{\partial z}=-\frac{1}{\rho}\frac{\partial p}{\partial x}-\frac{\partial}{\partial x}\overline{u^2}-\frac{\partial}{\partial z}\overline{uw}+\nu\nabla^2U \quad (2)$$

and

$$U\frac{\partial W}{\partial x}+W\frac{\partial W}{\partial z}=-\frac{1}{\rho}\frac{\partial p}{\partial z}-g-\frac{\partial}{\partial x}\overline{uw}-\frac{\partial}{\partial z}\overline{w^2}+\nu\nabla^2W. \quad (3)$$

Further, for the uniform homogeneous canopy, we assume horizontal parallel flow that is steady and homogeneous. Under these conditions, eq (2) and (3) simplify to

$$0=-\frac{1}{\rho}\frac{\partial p}{\partial x}-\frac{\partial}{\partial z}\overline{uw}+\nu\frac{\partial^2}{\partial z^2}U \quad (4)$$

and

$$0=-\frac{1}{\rho}\frac{\partial p}{\partial z}-g-\frac{\partial}{\partial z}\overline{w^2}. \quad (5)$$

Within the framework of the modeling assumptions, we can draw some conclusions regarding the pressure distribution. When differentiating eq (5) with respect to x,

$$\frac{1}{\rho}\frac{\partial^2 p}{\partial x\partial z}=-\frac{\partial^2}{\partial x\partial z}\overline{w^2}. \quad (6)$$

Because of x homogeneity, however, the statistical properties of the flow are independent of x; therefore, the right-hand side of eq (6) becomes zero, and

$$\frac{\partial^2 p}{\partial x\partial z}=\frac{\partial}{\partial z}\left(\frac{\partial p}{\partial x}\right)=0 \quad (7)$$

which yields $\partial p/\partial x$ as constant independent of z. Hence, as in the case of classical boundary layer flow, the pressure gradient of the outer flow is impressed into the canopy flow regime.

A further simplification of eq (4) by the neglect of a pressure gradient should be examined. There are two sources of pressure gradient effects that come to immediate attention. First is the large-scale pressure gradient that is the driving force for the flow. The magnitude of the acceleration from this pressure gradient is on the order of 10^{-4} m·s^{-2}. This results in negligible accelerations for the scales of interest.

Another pressure gradient effect is operative in nonhomogeneous regions, such as canopy transition zones where the horizontal flow is decelerated.

From eq (2), it is seen that $(\partial U/\partial x)<0$ implies $(\partial p/\partial x)>0$. This situation occurs in a leading edge transition where the horizontal wind component is observed to decelerate. Conversely, at a downwind transition, $(\partial U/\partial x)>0$; and the corresponding pressure gradient is negative. Briefly, then, the steady-state pressure field will show an increase with distance into the canopy. Pressure gradient cannot remain positive throughout a broad canopy without incurring unrealistic pressure values. It is reasonable to expect dynamic pressure to increase through the transition region but to reach a constant value in the equilibrium flow regime.

The details of the pressure variations have yet to be explored, but qualitative reasoning and empirical evidence suggest a basically smooth, asymptotic approach to the downstream constant value. Undoubtedly, there are perturbations superimposed on the smooth variation. These are related to the wave effect discussed in connection with the transition zone model. The simple x dependence of pressure suggested for the steady flow differs from the nonsteady mechanics. It is likely that time-dependent circulations occur when the local pressure buildup results in a separation of flow from the wall and consequent reversal of direction within the canopy. It is felt that these eddies are generally random in position and duration; and therefore, their effects do not show in the time-averaged or steady case.

The long downwind extent of the approach to uniform pressure conditions suggests that the ideal canopy, free of edge effects, may be rare indeed. For the uniform zone model, however, we shall consider only $\partial p/\partial x=0$.

In the upper layer, flow is maintained by turbulent and viscous shear stresses transferring momentum from the free stream flow. The molecular friction term is negligible everywhere except in a very thin laminar sublayer adjacent to the wall, and the viscous effects can be incorporated into a surface roughness parameter. The result is a further simplification of eq (4) to an expression for constant turbulent stress, $\overline{uw}$=constant. If the momentum mixing length concept is adopted, we ultimately obtain

$$\frac{dU}{dz}=\frac{u_*}{l(z)} \tag{8}$$

where u_* is the friction velocity. The total derivative notation is used since $U=U(z)$ only.

Having adopted the momentum mixing length concept, we can specify a form for the mixing length $l(z)$ and integrate. The boundary layer above a porous surface such as a canopy is characterized by $l(z) \propto z$. However, turbulent exchange and mixing length do not vanish at the canopy top:

$$\frac{dU}{dz}=\frac{u_*}{l_0+k(z-h)}, \quad z\geq h \tag{9}$$

where l_0 is the value of mixing length at the interface, $z=h$, and k is von Kármán's constant, 0.4. Integration from h to z gives

$$U(z)-U(h)=\frac{u_*}{k}\ln\left(\frac{l_0+k(z-h)}{l_0}\right), \quad z\geq h. \tag{10}$$

The flow in the inner layer is driven by the stress imposed at the interface and may be modeled as an extension of the flow between parallel moving plates. The problem of turbulent Couette flow between two parallel plates moving in opposite directions was studied by Reichardt (1956). The (constant) stress in the flow was expressed as the sum of a turbulent and laminar term in the form of

$$\tau=(\mu+A)\frac{dU}{dz} \tag{11}$$

where μ is the molecular viscosity of the fluid and A is an eddy viscosity that varies with distance from the walls.

The current model of canopy flow treats the shear flow between the moving interface and stationary ground surface. The momentum imparted to the interfacial surface by the upper flow is transferred in turn to the lower flow. Conditions at the interface are continuity of velocity, mixing length, and stress. At the lower surface, mixing length approaches zero.

In treating turbulent Couette flow, Reichardt used a parabolic distribution of eddy viscosity. An equivalent formulation, after using mixing length, will lead to a similar profile for l. Therefore, we hypothetically propose the following expression for mixing length:

$$l=r\left[\frac{h^2}{4}-\left(z-\frac{h}{2}\right)^2\right]+sz=-rz^2+(hr+s)z \tag{12}$$

where h is canopy height, r and s are parameters; r determines the maximum value for l, and s insures continuity of l at the interface.

The flow in the inner layer is described by eq (8). Substituting the mixing length expression (eq 12) and integrating, we obtain

$$U=\frac{u_*}{-(rh+s)}\left[\ln\left|\frac{z-\left(\frac{rh+s}{r}\right)}{z}\right|-\ln\left|\frac{z_0-\left(\frac{rh+s}{r}\right)}{z_0}\right|\right]. \tag{13}$$

From eq (12) we see that r and s are introduced as descriptors of the mixing length. The parameter s may be viewed as a secondary surface roughness and is related to the canopy density. The range of s values, as seen from the limiting cases, is 0 to 0.4 (von Kármán's constant). The other parameter r represents the maximum value of the parabolic term for canopy mixing length. The lower limit for r is zero (no canopy). Its upper limit, from dimensional and physical reasoning, should be on the order of the inverse of the canopy height.

The behavior of r can be approached through dimensional analysis. We make the hypothesis that r depends on canopy density, Λ^{-1} (length^{-1}); mean wind speed, U (length time^{-1}); and turbulent velocity, u (length time^{-1}). Then we obtain

$$rh \propto \phi_1\left(\frac{h}{\Lambda}, \frac{u}{U}\right). \tag{14}$$

We know $\lim_{\Lambda\to 0}\phi_1=1$ and $\lim_{\Lambda\to\infty}\phi_1=0$, but the remaining properties of ϕ_1 must be determined empirically. Similarly, dependence of s on the mean wind shear $\partial U/\partial z$, Λ, and U can be postulated; and we obtain

$$s \propto \phi_2\left(\frac{\Lambda}{U}\frac{\partial U}{\partial z}\right). \tag{15}$$

An interrelation is suggested by the result that sparse canopies imply high s and low r, and conversely. Simple functional forms that satisfy the limiting conditions for dependence on Λ are exponentials of the form

$$\phi_1 \propto e^{-\Lambda/h}, \quad \phi_2 \propto 0.4e^{-const/\Lambda}. \tag{16}$$

Figure 1 shows the domain of r and s derived using assumed exponentials.

One aspect in which our model differs from those of other investigators is that a maximum in the mixing length

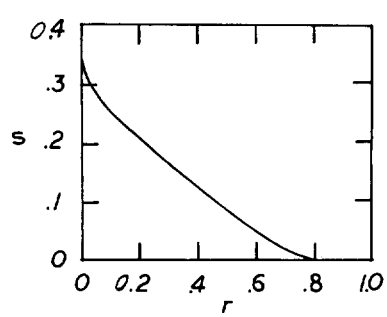

FIGURE 1.—Expected domain of velocity profile parameters r and s.

profile lies within the canopy. Previous theories postulate a mechanical breakdown of turbulent eddies leading to a nearly uniform mixing length within the canopy. At this point, we should remember that mixing length is a parameter of one theory of turbulent transport. In a sense, the mixing length implies an efficiency of turbulence transport by all available processes. If the environment induces a new turbulent transfer mechanism, this would be reflected in the mixing length parameter. Hypotheses on the parameter made without considering all the physical mechanisms could then be in error.

The vegetative canopy environment is capable of producing many aerodynamic effects besides the often-considered ones of frictional drag and mechanical eddy breakdown. One such effect noted by Yano (1966) is that a cylinder of finite length placed in a flow gives rise to a distinctly three-dimensional wake. The velocity deficit in the lee of the obstacle is countered by momentum transport, not only normal, but also parallel to the axis. The effect of flow over the end of a cylindrical obstacle is likely to be greater if the cylinder projects from a wall into a shear flow, as in the case of a tree in the atmosphere. Yano also finds the effect to carry over to an ensemble of elements.

SUMMARY

The modeling of canopy flows almost certainly necessitates the consideration of interaction between two regimes. In the steady, horizontally homogeneous case, the interaction can be handled by matching solutions for the two layers at the interface. In the present model, we have proposed an interaction of a boundary layer flow with a turbulent Couette flow and have been able to produce the main features of observed canopy wind fields. Perhaps the most important point is that we were able to derive the model equations directly from the governing equations, assuming only the mixing length parameter of turbulent exchange. A test of this assumption, using the energy balance equation, was favorable.

Although we have been able to suggest theoretical dependencies of r and s on canopy density and wind speed, the test of the model will come from future empirical validation. Figure 2 shows sample profiles for several combinations of parameters. We do not intend, however, to stress the curve-fitting abilities of the profiles. The model is primarily designed to provide a boundary condition for the transition zone model discussed in the next section. It satisfies the same governing equations and describes the velocity field in terms of simple functions. Its immediate use, then, is as a theoretical tool to explore a more complex wind field.

3. TRANSITION ZONE MODEL

The assumption of parallel flow, which is quite valid for modeling the flow in the uniform zone, does not hold in the transition zones near the upwind and downwind edges of a canopy. Field and laboratory observations all show significant vertical motions in these regions.

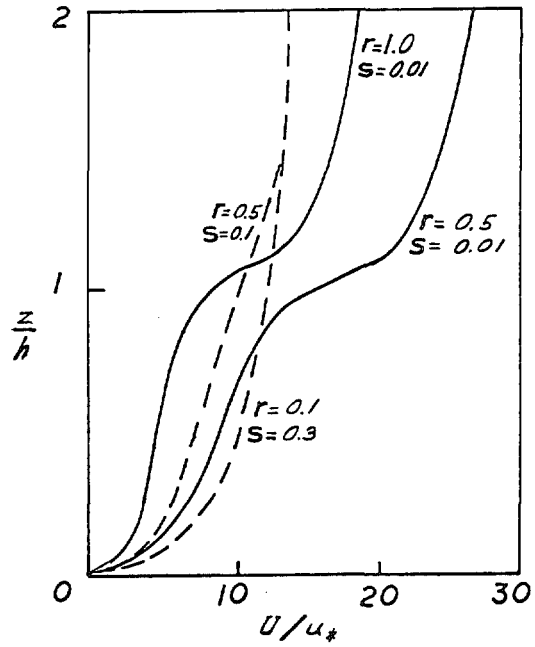

FIGURE 2.—Sample velocity profiles for equilibrium canopy flows.

For studying the properties of flow in the transition zones, a two-dimensional model has been developed. In formulating the model, we begin with the vorticity equation obtained by subtracting the x derivative of eq (3) from the z derivative of eq (2). We assume steady flow of homogeneous, incompressible fluid. The resulting form of the continuity equation is

$$\frac{\partial U}{\partial x}+\frac{\partial W}{\partial z}=0. \tag{17}$$

Also, we assume that viscous effects are negligible compared with Reynolds stresses. Hence, in addition to the continuity equation, the equation governing the flow is

$$U\frac{\partial \zeta}{\partial x}+W\frac{\partial \zeta}{\partial z}=\frac{\partial^2}{\partial z\partial x}(\overline{u^2}-\overline{w^2})+\left(\frac{\partial^2}{\partial z^2}-\frac{\partial^2}{\partial x^2}\right)\overline{uw}. \tag{18}$$

If we adopt the mixing length hypothesis to relate the Reynolds stress to the mean velocity profile, we get

$$\overline{uw}=-l^2\left|\frac{\partial U}{\partial z}\right|\frac{\partial U}{\partial z}. \tag{19}$$

Empirical evidence suggests that the first term on the right-hand side of eq (18) may be small compared with the other terms. In the present model, it will be neglected.

The continuity equation can be incorporated into the vorticity equation through the use of a stream function defined such that

$$U=\frac{\partial \psi}{\partial x},\quad W=-\frac{\partial \psi}{\partial x}. \tag{20}$$

When we make these changes in eq (18), we obtain

$$\frac{\partial \psi}{\partial z}\frac{\partial \zeta}{\partial x}-\frac{\partial \psi}{\partial x}\frac{\partial \zeta}{\partial z}=\left(\frac{\partial^2}{\partial x^2}-\frac{\partial^2}{\partial z^2}\right)l^2\left|\frac{\partial^2 \psi}{\partial z^2}\right|\frac{\partial^2 \psi}{\partial z^2}; \tag{21}$$

and as a consequence of the definitions of ψ and ζ,

$$\zeta=-\left(\frac{\partial^2\psi}{\partial x^2}+\frac{\partial^2\psi}{\partial z^2}\right). \tag{22}$$

Equations (21) and (22) make up a nonlinear set of partial differential equations that may be solved subject to a set of boundary conditions. Because of the nonlinearity, the equations must be solved by numerical methods.

A two-layer model has been set up in which the lower layer represents the region below the canopy top and the upper layer represents the outer flow. The boundary conditions at the ends of the regions are the vorticity and stream function corresponding to the parallel flows for the upwind and downwind environment. That is, for the leading edge transition, the upstream conditions are consistent with the logarithmic velocity profile; and the downstream conditions are represented by the canopy flow discussed in the previous section. At the downstream edge, the end conditions are reversed. At $z=z_0$, the lower boundary conditions are

$$W=0,\ U=0,\ \text{and}\ \psi=0$$

where z_0 is a specified surface roughness parameter. At the top of the upper region, ψ is specified; and at the interface between the two layers, the solutions are matched by requiring that shearing stress and stream function be continuous.

It is seen from the previous section that the parameters determining both the upstream and downstream uniform flows are $l(z)$, u_*, and z_0. A requirement in the model is the specification of $l(x,z)$ and $z_0(x)$ across the transition zone. The shear stress at the lower surface must also be specified. In the absence of definitive information on the variation of these parameters in a transition zone, it was decided to vary them smoothly from one equilibrium value to the other. A weighting function is defined for this purpose as

$$A(x)=\frac{1}{2}\left[1-\tanh\left(bx+c\right)\right] \tag{23}$$

The parameter b allows a variation in the width of the mixing length transition zone, while c merely places the zone in the desired portion of the grid network. Dimensionally, b should be related to the inverse of the spacing between roughness elements with a suggested proportionality constant of about 0.4.

FINITE-DIFFERENCE GRID

The grid upon which the calculations are performed consists of two separate units, 11 grid points vertically by 21 grid points long, placed one above the other. The values of the variables in the bottom row of the upper grid are set equal to those on the top row of the lower grid. The spacing of the grid points can be varied, but useful values were found to be $z=0.1\ h$, $x=5\ h$ where h is the canopy height.

NUMERICAL PROCEDURE

The procedure for solving the set of eq (21) and (22) can be outlined as follows.

1. Define the end boundary conditions using eq (10) and (13) with the desired parameters. Note that the equations are expressed in dimensionless form, the scaling parameters being u_* for velocity and h for length.

2. Express initial estimates of the variables ψ, ζ and calculate mixing length across the grid in terms of the end quantities weighted by $A(x)$.

3. Calculate the left-hand side of eq (21) for each interior grid point from the current estimates of ψ, ζ using

$$F_{i,j}=\frac{1}{4\Delta x\Delta z}\left[(\psi_{i,j+1}-\psi_{i,j-1})(\zeta_{i+1,j}-\zeta_{i-1,j})-(\psi_{i+1,j}-\psi_{i-1,j})(\zeta_{i,j+1}-\zeta_{i,j-1})\right]. \tag{24}$$

4. Solve

$$\left(\frac{\partial^2}{\partial x^2}-\frac{\partial^2}{\partial z^2}\right)\varphi=F(x,\,z) \tag{25}$$

where

$$\varphi=l^2\left|\frac{\partial^2\psi}{\partial z^2}\right|\frac{\partial^2\psi}{\partial z^2}$$

by a marching procedure

$$\varphi_{i,j+1}=-\varphi_{i,j-1}+2\varphi_{i,j}+\left(\frac{\Delta z}{\Delta x}\right)^2(\varphi_{i+1,j}+\varphi_{i-1,j}-2\varphi_{i,j})-\Delta z^2F_{i,j}. \tag{26}$$

5. Calculate $\partial^2\psi/\partial z^2$ from φ by

$$\left(\frac{\partial^2\psi}{\partial z^2}\right)_{i,j}=\frac{\sqrt{\varphi_{i,j}}}{l_{i,j}}\,\text{sgn}\,(\varphi_{i,j}) \tag{27}$$

where $\text{sgn}(\varphi_{i,j})$ has the value $+1$ or -1 depending on the sign of $\varphi_{i,j}$.

6. Calculate ψ from the values of $\partial^2\psi/\partial z^2$ and upper and lower boundary conditions on ψ. The Liebmann sequential overrelaxation method (Thompson 1961) is applied separately for each x value.

7. The next step in the procedure is to update the boundary conditions on the interface between the two layers. This is necessary to allow the interacting flows to develop without too many artificial constraints.

8. The interior ζ values are calculated from the ψ field by the equation

$$\zeta_{i,j}=\frac{-1}{\Delta x^2}(\psi_{i+1,j}+\psi_{i-1,j}-2\psi_{i,j})-\frac{1}{\Delta z^2}(\psi_{i,j+1}+\psi_{i,j-1}-2\psi_{i,j}). \tag{28}$$

9. Return to step (3). Steps (3) through (8) are repeated until the convergence criterion is reached.

DISCUSSION OF ACCURACY, TRANSITION ZONE MODEL

The question of accuracy in the transition zone model is mainly that of numerical errors and the approximations in the defining equations.

Major restrictions in the model are the assumptions made in deriving the governing equations, and the most severe of these is the neglect of a horizontal eddy viscosity. It should be recalled that, in deriving eq (21), we assumed that stress was approximated by $l^2|(\partial U/\partial z)|(\partial U/\partial z)$ and neglected turbulent transport arising from horizontal velocity gradients. This is tantamount to assuming that horizontal variations in wind speed are negligible in comparison with vertical variations. While this is rigorously true of horizontal flows, it is only approximate in the transition zone. The extent of approximation is difficult to judge due to the lack of information on the horizontal mixing properties but may be estimated by means of scale analysis. If we assume the total stress to be given by two components, horizontal and vertical, we can rewrite eq (21) as

$$\psi_z\zeta_x-\psi_x\zeta_z=\left(\frac{\partial^2}{\partial x^2}-\frac{\partial^2}{\partial z^2}\right)[l_x^2|\psi_{xx}|\psi_{xx}+l_z^2|\psi_{zz}|\psi_{zz}]. \quad (29)$$

Take the characteristic scales, velocity$=U$, horizontal length$=L$, vertical length$=\lambda$. Further assume $O(l_x)=O(l_z)=\lambda$. Then, expressing the terms of eq (29) as scaled quantities and simplifying, we obtain the magnitudes of the terms:

$$\psi_z\zeta_x-\psi_x\zeta_z=\frac{\partial^2}{\partial x^2}(l_x^2\varphi_x)-\frac{\partial^2}{\partial z^2}(l_x^2\varphi_x)+\frac{\partial^2}{\partial x^2}(l_z^2\varphi_z)-\frac{\partial^2}{\partial z^2}(l_z^2\varphi_z). \quad (30)$$

$$1 \qquad \frac{\lambda^3}{L^3} \qquad \frac{\lambda}{L} \qquad \frac{\lambda}{L} \qquad \frac{L}{\lambda}$$

We simplify notation; thus $|\psi_{xx}|\psi_{xx}=\varphi_x$, and similarly for φ_z. The last two terms on the right-hand side are retained in the present model, while the first two are neglected. The ratio of the first to the fourth term on the right is λ^4/L^4, while the ratio of the second to the fourth term is λ^2/L^2. Typical values of λ/L for transition zone calculations are between 0.25 and 0.01. We can see from this that the errors introduced by neglecting horizontal mixing can approach 6 percent for narrow transition zones but remain negligible for wide zones.

The other term neglected from eq (18) was $(\partial^2/\partial x\partial z)(\overline{u^2}-\overline{w^2})$ that depends on the spatial variation of $\overline{u^2}$ and $\overline{w^2}$. From empirical observation, the total change in $(\overline{u^2}-\overline{w^2})$ from inside to outside the canopy is on the order of $0.2\ u_*$. Scaling the term by characteristic length scales and comparing it with the above, we find a ratio of 0.2 λ/L that suggests errors of 5 percent and less introduced by neglect of this term.

The various numerical subprocedures each have accuracy limits; but in general, they may be kept to a desired level well within the tolerances set up by the assumptions in the governing equation. The biggest numerical error is the truncation error associated with the finite-difference estimate of derivatives. This is done in the calculation of the Jacobian term in step (3) and in step (8), which is the calculation of the vorticity from the stream function. Typical bounds on this error are 0.3 percent per iteration.

Although the truncation errors for a single iteration are relatively small, they have a cumulative effect; and there is some point at which the truncation error will limit the convergence of the scheme. This is best determined by analyzing the convergence criteria from step to step. The criteria selected were the maximum changes in ζ and ψ over the entire grid from one iteration to the next. The general pattern is a decrease in these changes for about 20 iterations after which they level off or increase. This behavior was interpreted as the influence of accumulated truncation error, and the procedure was stopped at this point. Another test was made on the stability of the solutions. The results for the case $b=\infty$ were compared after 20 and 40 iterations and were found to differ only in minor aspects. Maximum ψ differences were approximately 5 percent between the two patterns.

In summary, the transition zone model must be considered an approximation with expected errors $|\psi_{est}-\psi|/|\psi|$ on the order of 6 percent for sharp transitions and less than that for broad transition zones.

TRANSITION MODEL RESULTS

The transition zone model has been applied to a typical case. The boundary condition for canopy flow is given by eq (10) and (13) with parameters $z_0=0.01\ h$, $s=0.01$, $r=1.0$. The outer flow boundary conditions are expressed by the familiar logarithmic velocity profile

$$U(z)-U(z_0)=\frac{u_*}{k}\ln\left|\frac{z}{z_0}\right| \quad (31)$$

with parameters $z_0=0.01\ h$, $U(z_0)=0$. The stream function was maintained essentially constant at the top row of the grid giving horizontal flow there. This requirement has a damping effect on vertical motions generated within the grid.

Calculations were performed for a wide range of values of the parameter b and represent transition zone widths from 1 to 100 times the canopy height. Figures 3 and 4 show the computed streamlines for $b=0.5$ and ∞ at the leading edge of a canopy. It can be seen that, as the transition becomes sharper, the pattern of vertical motions becomes more distinct. One of the more striking features of the results is the large downstream distances at which the windward edge effects are still present. Regardless of the value of b, effects are noticeable at 50 to 60 canopy heights downwind.

The patterns in figures 3 and 4 will be described briefly to point out important features. The flow above $h/2$ rises at or slightly downstream from the leading edge. The steepness of this rise depends on b. At $x=15\ h$, there is a peak; and the streamlines dip back down, reaching a minimum at $x=25\ h$ to $30\ h$. The vertical motions are most distinct just above the top of the roughness elements. Beyond the dip, there is another wave of slightly smaller amplitude with the second dip at 50–60 h. This pattern is superimposed on a set of streamlines that rises smoothly from upstream to downstream end conditions. Meanwhile, in the lower half of the canopy, the flow does not rise at the

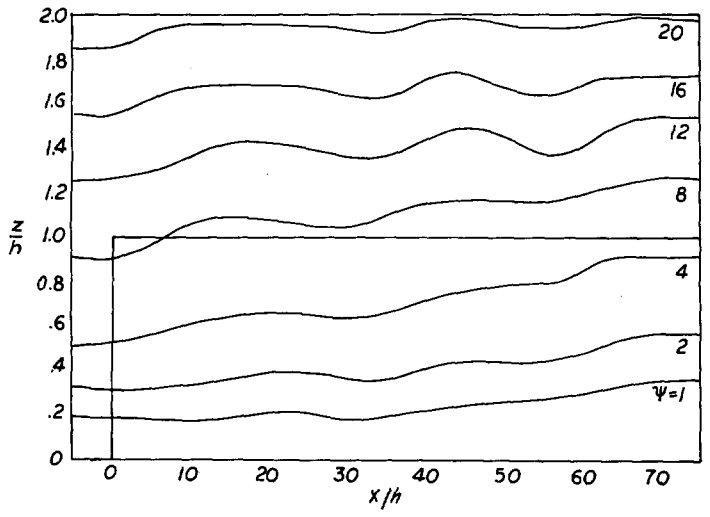

FIGURE 3.—Leading edge streamline pattern, $b=0.50$.

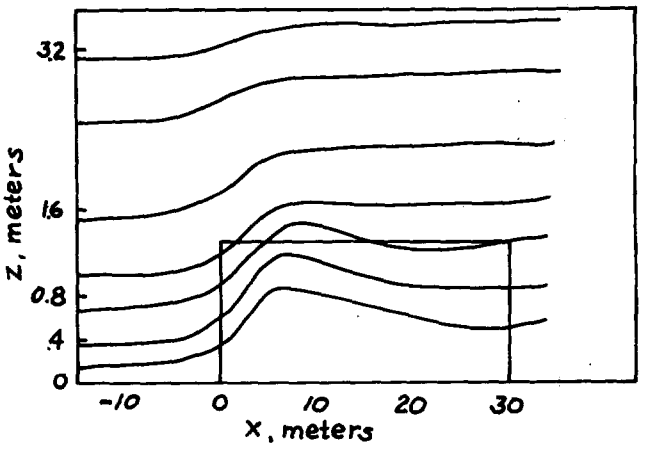

FIGURE 6.—Streamlines based on observed data presented by Stearns (1964), case of Mar. 11, 1964.

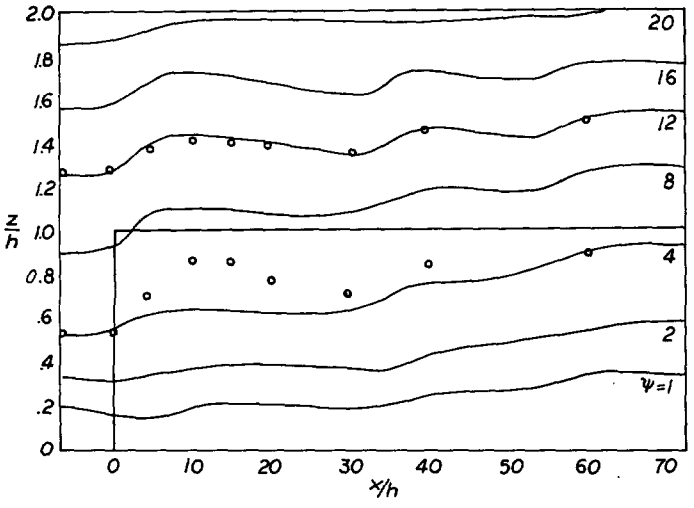

FIGURE 4.—Leading edge streamline pattern, $b=\infty$ (step change).

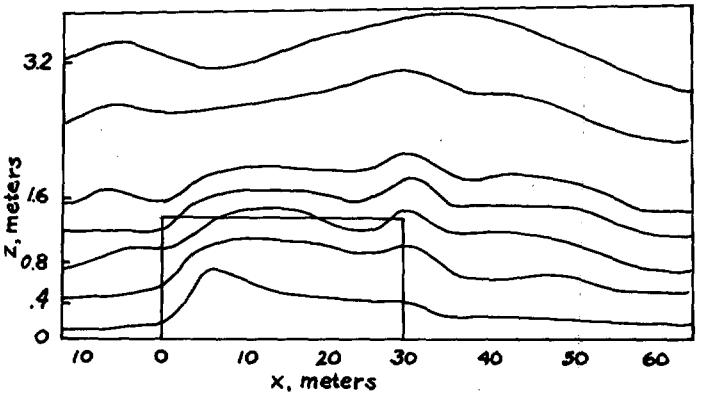

FIGURE 7.—Streamlines based on observed data presented by Stearns (1964), case of Mar. 12, 1964.

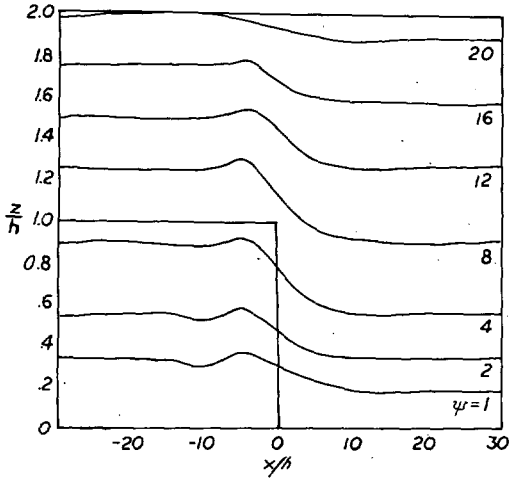

FIGURE 5.—Trailing edge streamline pattern, $b=1.0$.

leading edge but rather sinks to a weak minimum at about $x=5\,h$ before conforming to a much damped version of the pattern described above. Streamlines for the downwind edge are shown in figure 5 for $b=1.0$. In general, the trailing edge flow is smoother than that at the leading edge. The main features are a downward slope to the streamlines for all b (not shown); but at high b values (i.e., $b=1.0$), a superposed wave creates a dip followed by a peak just prior to the trailing edge. No significant downstream effects occurred in the calculations.

There are several sources of empirical data available for comparison with the model, although all are from finite-length canopies, and hence not strictly comparable. Stearns (1964) measured velocity profiles at several distances across a model canopy in the atmosphere. Stream functions were calculated from Stearns' winds, and the streamline patterns subsequently derived are shown in figures 6 and 7. Recently, Meroney et al. (1968) and Kawatani and Meroney (1968) reported similar results from wind tunnel simulations for forest canopies that included streamline patterns.

Agreement between the characteristics of the computed and observed streamlines is quite striking. In both empirical sets, the sharpest rise occurs slightly downwind of the edge of the canopy. Beyond this, there is a tendency for the flow to return to horizontal or actually curve downward. Stearns' model is likely too short to observe downstream effects, but the wind tunnel canopy (not shown) indicates a dip about $x=25\ h$, which is most distinct near the canopy top. A second, much weaker node appears at $x=60\ h$ to $70\ h$. For sparser canopies, the wave effect observed by Meroney et al. (1968) is of smaller amplitude with a suggestion of longer wave length. The wave pattern in the wind tunnel streamlines is superimposed on a mean pattern. Rather than leveling off the streamlines continue to rise along the entire length of the model. This suggests a continued downwind pressure change within the model. As the trailing edge is approached, there is a final wave-type deflection in the flow and indications of a downward motion behind the canopy. Stearns' data show the same effect at the downwind edge—a remarkable agreement with figure 5. Quantitative comparison with the observations of Kawatani and Meroney is obtained for the leading edge streamlines. Since the boundary conditions in the numerical model are slightly different from those of the wind tunnel experiments, the magnitudes of the streamline deflections differ. The two data sets were reduced to the same scale through normalization by the total height deflection of the streamline between upwind and downwind boundaries. Observed data points reduced in this manner are included in figure 4 for two typical streamlines. The agreement above the canopy top is remarkable for all distances. Within the canopy, although the wave length is the same, the observations show a greater amplitude in the initial rise.

Another minor feature is the splitting effect in which the flow entering the lower portion of the canopy sinks instead of rises. This phenomenon is a pertinent one for prototype applications and has been observed in the diffusion of suspended material. Raynor (1967) shows concentration measurements from a tracer released upstream of a forest. There is a distinct splitting of the cloud as the portion that enters the canopy close to the ground stays there while that entering higher tends to rise. The splitting of the flow is also very evident in velocity profiles taken in the field. The results of virtually all mean wind profile measurements in upwind canopy transition zones show a weak maximum within the canopy. Associated with this is a tendency for jetting above the roughness elements. Although no maximum may occur, the effect shows up as a zone of strong velocity shear between zero and $10\ h$ units downstream of the leading edge. The shear region diminishes further downwind.

To compare these effects with the model results, we calculated the horizontal and vertical velocity components from the stream function by means of the defining eq (20). The profiles of horizontal velocity U for two b values have been selected for discussion. The case of sharpest transition (fig. 8) shows the effects most clearly. There is a slight tendency toward velocity increase in the lowest one-tenth of the canopy very near the leading edge. Meanwhile, a distinct jet forms just above the canopy top. These effects disappear by the next column of grid points, $5\ h$ downstream. The same phenomenon occurs at the next downstream node as is shown by profiles at $x=32\ h$ and $x=37\ h$. The profiles for $b=0.5$ (fig. 8) show a strongly diminished tendency for the formation of jets, although the effect can still be seen. The U profiles at the downwind edge do not display the jetting effects.

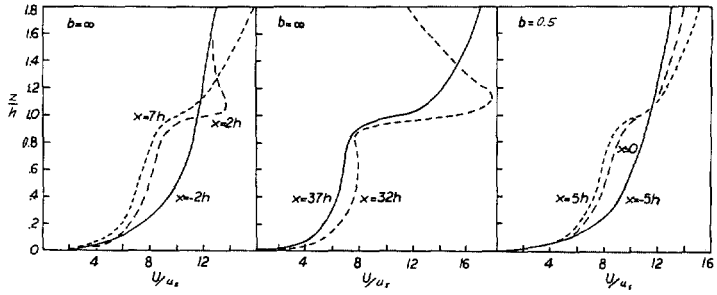

FIGURE 8.—Mean velocity profiles at several distances from a canopy leading edge.

The transition model has been derived to explain the two-dimensional effects in the wind variation near the edges of canopies. The practical requirements for this type of information are important since most natural sites are subject to edge effects.

Through a systematic approach beginning from the basic equations, we have been able to estimate the errors involved in the simplifying assumptions and numerical procedures. The model quite adequately describes several observed phenomena associated with transition zone flow including wave and splitting effects. In addition, the results suggest the presence of features not observed. The long downwind distances at which leading edge influences appear is notable, although not really surprising. A second wave suggested by the calculations may have minor practical implications but represents a significant aspect of the fluid mechanics.

4. SUMMARY AND CONCLUSIONS

The development of a model for flow in the transition regions of vegetative covers is vital for almost every practical application depending on wind and turbulence structure. Edge effects appear to penetrate far enough into interior regions, so that examples of perfectly uniform canopy flow are scarce. Our approach to a transition model has been first to establish a model for a uniform cover that is consistent with the equations governing the two-dimensional transition flow. It was shown that the traditional model (eq 1) implies a complex height de-

pendence of pressure, whereas the Reynolds equations of motion for the same regime allow no more than a linear variation. A uniform canopy model was developed from the equations of motion, making use of mixing length theory and a hypothesis of two-layer flow interaction.

The uniform model provided a boundary condition for the two-dimensional steady nonlinear transition flow obtained numerically. Several simplifying assumptions have been made in the transition zone model. Although the effects have been estimated to be an order of magnitude less than the included effects, the role of these terms will be examined in later models. The neglected processes include horizontal mixing, vertical variation of turbulence anisotropy, and, of course, the role of the third (lateral) dimension. Also, further experiments on upper boundary conditions are necessary to make this a practical model.

The simplified model yielded several interesting flow features that verified well against observation when adjustments for differing boundary conditions were made. Features such as a splitting of the flow at the leading edge with a weak velocity maximum within the canopy occur in both the calculations and observations. Also, a standing wave in which the air is forced up at the canopy edge and dips back into the cover some distance downwind verifies semiquantitatively with wind tunnel data.

A logical use of the model is in the study of transport and diffusion of suspended material in the canopy environment. In addition to the two-dimensional transport obtained directly, the momentum diffusivity implied in the model design can be extended to include turbulent transfer of scalar quantities. Also, the use of models in the design of experiments and field studies frequently leads to more meaningful experimental results.

ACKNOWLEDGMENTS

I am grateful to Dr. S. -K. Kao of the University of Utah for his helpful suggestions and discussions.

REFERENCES

Allen, Luther H., Jr., "Turbulence and Wind Speed Spectra Within a Japanese Larch Plantation," *Journal of Applied Meteorology*, Vol. 7, No. 1, Feb. **1968**, pp. 73–78.

Baynton, Harold W., Biggs, W. Gale, Hamilton, Harry L., Jr., Sherr, Paul E., and Worth, James J. B., "Wind Structure in and Above a Tropical Forest," *Journal of Applied Meteorology*, Vol. 4, No. 6, Dec. **1965**, pp. 670–675.

Cionco, Ronald M., "A Mathematical Model for Air Flow in a Vegetative Canopy," *Journal of Applied Meteorology*, Vol. 4, No. 4, Aug. **1965**, pp. 517–522.

Inoue, Eiichi, "On the Turbulent Structure of Airflow Within Crop Canopies," *Journal of the Meteorological Society of Japan*, Ser. 2, Vol. 41, No. 6, Tokyo, Dec. **1963**, pp. 317–326.

Kawatani, Takeshi, and Meroney, Robert N., "The Structure of Canopy Flow Field," *Technical Report*, Grant No. DA–AMC–28–043–65–G20, Fluid Dynamics and Diffusion Laboratory, Colorado State University, Ft. Collins, Aug. **1968**, 122 pp.

Lemon, Edgar R. (Editor) et al., *The Energy Budget at the Earth's Surface: Part II. Studies at Ithaca, N.Y., 1960, Production Research Report* No. 72, U.S. Agricultural Research Service, Ithaca, N.Y., Sept. **1963**, 49 pp.

Meroney, Robert N., "Characteristics of Wind and Turbulence in and Above Model Forests," *Journal of Applied Meteorology*, Vol. 7, No. 5, Oct. **1968**, pp. 780–788.

Meroney, Robert N., Kesic, D., and Yamada, T., "Gaseous Plume Diffusion Characteristics Within Model Peg Canopies: Task IIB Research Technical Report, Deseret Test Center," *Technical Report* ECOM–C–0432–1, Contract No. DAAB07–68–C–0423, U.S. Army Electronics Command, Ft. Monmouth, N.J., Sept. **1968**, 70 pp.

Morton, John, "Subtropical Rain Forest Diffusion Study," paper presented at the American Meteorological Society Conference on Fire and Forest Meteorology, Salt Lake City, Utah, Mar. 12–14, **1968**.

Plate, E. J., and Quraishi, A. A., "Modeling of Velocity Distributions Inside and Above Tall Crops," *Journal of Applied Meteorology*, Vol. 4, No. 3, June **1965**, pp. 400–408.

Raynor, Gilbert S., "Effects of a Forest on Particulate Dispersion," *Proceedings of the U.S. Atomic Energy Commission Meteorological Meeting, Chalk River Nuclear Laboratories, Ontario, Canada, September 11-14, 1967*, Atomic Energy of Canada, Ltd., Ontario, **1967**, pp. 581–588.

Reichardt, Hans, "Uber die Geshwindigkeitsverteilung in Einer Geradlinigen Turbulenten Couette Stromuing" (On Velocity Distribution in Rectilinear Turbulent Couette Flow), *Zeitschrift für Angwandte Mathematik und Mechanik*, Vol. 36 Supplement S, Berlin, Germany, Sept. **1956**, pp. S–26—S–29.

Shinn, Joseph H., "Air Flow in the Tree Trunk Region of Several Forests," paper presented at the National Meeting of the American Meteorological Society With the Pacific Division, American Association for the Advancement of Science, Logan, Utah, June 26–28, **1968**.

Stearns, Charles R., "Report on Wind Profile Modification Experiments Using Fields of Christmas Trees on the Ice of Lake Mendota," *Annual Report*, Contract No. DA–36–039–AMC–00878, Department of Meteorology, University of Wisconsin, Madison, June **1964**, 115 pp.

Tan, H. S., and Ling, S. C., "Quasi-Steady Micro-Meteorological Atmospheric Boundary Layer Over a Wheatfield," *The Energy Budget at the Earth's Surface: Part II. Studies at Ithaca, N.Y., 1960 Production Research Report* No. 72, Agricultural Research Service, Ithaca, N.Y., Sept. **1963**, pp. 7–12.

Thompson, Philip Duncan, *Numerical Weather Analysis and Prediction*, Macmillan Co., New York, N.Y., **1961**, 170 pp.

Uchijima, Zenbei, and Wright, James L., "An Experimental Study of Air Flow in a Corn Plant-Air Layer," *Bulletin of the National Institute of Agricultural Sciences*, Ser. A, Vol. *II*, Tokyo, Japan, Feb. **1964**, pp. 19–65.

Yano, Motoaki, "Turbulent Diffusion in a Simulated Vegetative Cover," *Technical Report*, Grant No. DA–AMC–28–043–65–G20, Department of Civil Engineering, Colorado State University, Ft. Collins, May **1966**, 149 pp.

[*Received May 15, 1970; revised August 5, 1970*]